Duck-Billed Nematodes: What Microscopy Reveals about Dead Dinosaurs

Kersten Peterson,[1] Keith Holcomb,[2] and Mark Armitage[3]*

[1]Research Associate, DSTRI, Inc., Vader, WA
[2]President, DSTRI, Inc., Mansfield, TX
[3]Senior Microscopist, DSTRI, Inc., Sequim, WA

*profmark@dstri.org

Abstract: Nematodes are diverse microscopic worms that inhabit soils worldwide and play critical roles in decomposition and nutrient recycling. They are particularly important in the breakdown of vertebrate carcasses and are frequently recovered from soil environments associated with decaying organic material. Fossil nematodes have been reported from ancient sediments, amber, and occasionally from the internal structures of dinosaur bones. In this study, living nematodes were extracted from the vascular canals of dinosaur bones using a standard nematode extraction technique designed to recover viable organisms from soil matrices. Scanning electron microscopy (SEM) was then used to characterize these organisms, providing the first high-resolution morphological examination of nematodes associated with dinosaur bone microenvironments. These observations suggest that dinosaur bone may serve as a unique ecological niche for modern soil nematode communities. Further investigation of these communities, including taxonomic identification and ecological analysis, will be necessary to understand their origin, diversity, and potential ecological roles.

Keywords: *Edmontosaurus*, *Triceratops*, *Nanotyrannus*, fungivore, living opportunistic nematode

Introduction

Nematodes are extremely widespread and abundant organisms, inhabiting nearly every type of global soil including those in extreme environments [1–5]. They are found in high numbers in sub-Arctic regions, with highest densities in boreal forests across Russia, Scandinavia, and North America [1–5]. Nematodes comprise an estimated 80% of all multi-cellular organisms found in soil and are essentially aquatic, inhabiting the water film between soil particles [3]. They play an important role in decomposition, especially vertebrate carcasses where they invade within the first week after death (the fresh to bloated stages) [5–8].

It is known that cadaver presence on or within soils affects population and diversity of soil microorganisms, especially nematodes, because nutrient-rich "resource pulses" enter the soil often at the expense of other microorganisms [5–8]. Fungi and nematode populations (particularly bacterivores) are notably dominant within and around decaying bones [5–8].

Nematodes are represented in the fossil and archaeological record through multiple preservation pathways, such as amber, fossil stone, sandy sediments, chert, silicates, and coprolites. Juvenile and adult worms and even nematode eggs from dogs have been discovered [9–14]. A possible nematode ichnofossil has also been described from the gut contents of *Brachlophosaurus canadensis* from MT [15].

In 2022, we reported the discovery of nematodes in 40μm ground sections of *Nanotyrannus* and *Triceratop*s [16] (Figures 4 and 8) collected at the Hell Creek in MT. In a larger study in 2024 [17], we reported many nematodes in ground sections of *Nanotyrannus, Triceratops*, and *Edmontosaurus annectens* bones from the same location. At that time, we made note of a work that had described similar structures from 40μm ground sections within the vascular canals of a *Titanosaurus* fibula collected in Brazil [18]. That report described these fusiform shapes as "blood parasites" that died with the animal and were fossilized within bone canals, however, those shapes match the morphology of preserved extant nematodes from our own ground section work [16,17]. Essentially, they match 5 parameters of our discoveries; all were found in vascular canals, with dark grey to slightly green fusiform shape, irregular anisotropy, one or more tapered end, and dark internal oval spots [16,17]. Aureliano et al. admit that the fusiform shapes are much larger than typical blood parasites and add, "Size is in excess for most of the protozoan parasites," [18]. They are also markedly larger than the nematodes of the family *Onchocercidae*. No fossil examples of that group have been reported.

Furthermore, nematodes are now often found in decalcification solutions of *Triceratops* and *Nanotyrannus* bones that we process routinely from the Hell Creek formation (Figures 1 and 2) and in bone extraction experiments employing the Baermann funnel method, a classical nematology technique (Figure 3). Figure 3 shows a bone nematode identified as a fungus-consuming worm (fungivore) by an expert (J. Eisenback, personal communication). We also note that the nematodes in bone canals (fusiform shapes) are always associated with clotted blood material (Figures 4 and 5) because they were alive and feeding when the bones were immersed in fresh fixative (10% formalin) at the dig. This preserved them in place in the bone canals with apparent internal structure (Figure 5), although their cuticle is resistant to infiltration [17]. We therefore maintain that these fusiform-shaped nematodes were misidentified and represent novel dinosaur bone nematodes [16,17].

There continues to be growing evidence of fossilized microbial communities within dinosaur bone including the presence of extant bacteria [19,20], fungi [16,19–22] (Figure 5a), nematodes [16,17,21–24], and insect cadaver remains [24]. These microscopic decomposers appear to be actively recycling original bone and soft tissues within bones [25–27]. Discoveries

Figure 1: Unidentified nematode (brightfield) within decalcification solution of *Triceratops* condyle collected at Hell Creek formation, Glendive, MT. Scale bar=10μm.

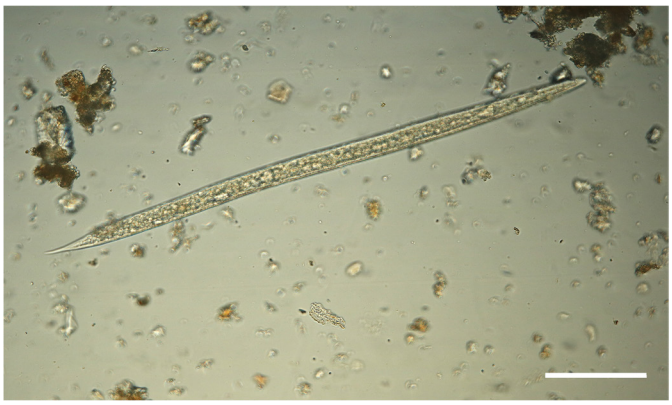

Figure 2: Unidentified nematode (brightfield) within decalcification solution of *Nanotyrannus* vertebra collected at Hell Creek formation, Jordan, MT. Scale bar=25μm.

Figure 3: Identified nematode (fungivore, DIC) within decalcification solution of *Triceratops* post-cranial shard collected at Hell Creek formation, Glendive, MT. Scale bar=75μm.

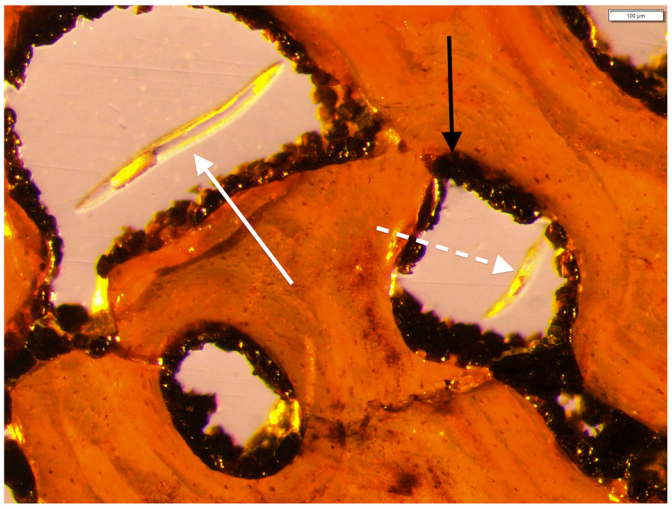

Figure 4: 40μm ground section of *Edmontosaurus annectens* femur vascular canal, (dissecting microscopy). Blood clot material is visible circumscribing the canal (black arrow). One adult nematode (white arrow) and one juvenile nematode (white dotted arrow) are visible within canals. Scale bar=100μm.

like this are rare and extraordinary, and little is known about how these communities are using the resources that obviously exist in dinosaur bone. Investigation of the specifics of what species are involved, how they consume bone resources, and their population dynamics is warranted.

With respect to "the most plentiful dinosaur remains recovered to date," there is some disagreement about which dinosaur is most represented, especially at the concurrently deposited Hell Creek and Lance formations of North America. Many consider *Tyrannosaurus rex* to be the obvious answer, however *E. annectens* certainly ranks highly (second to *Triceratops* and followed by *T. rex*) for sheer numbers of specimens recovered [28,29]. It is noteworthy that few reports of decomposers in hadrosaurs have been made from the 149 or so associated, articulated, and

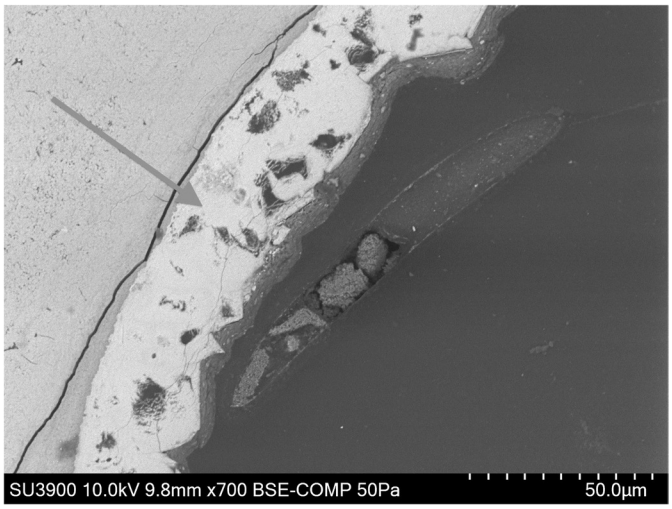

Figure 5: 40μm ground section (uncoated) of *Triceratops* condyle vascular canal, scanning electron microscopy (SEM-BSE). Blood clot material is visible circumscribing the canal (gray arrow). One adult nematode is visible within the canal, appressed to the clot material. Scale bar=50μm.

Figure 6: Partially buried *Edmontosaurus annectens* femur, located in the Lance formation, Hansen Ranch, Newcastle, WY. Left side of femur is heavily eroded. Scale marker on overburden slab=11cm on each side.

reported fossils of this organism, or the 41,000 isolated bones that have also been tabulated. (These numbers do not include private collections or those from museums, teaching centers, and such.) A whopping 46% of those belong to the hadrosaur clade [28]. It might also be argued that hadrosaurs are the most studied dinosaurs, especially with so many specimens examined histologically [30,31], but only *Centrosaurus* has been shown to harbor living bacteria [20,31]. Only recently has the presence of nematodes inhabiting the bones of *Triceratops, Nanotyrannus,* and *Edmontosaurus* been reported [16,17,21–24].

This study investigates whether fossilized dinosaur bone from *Edmontosaurus annectens* can harbor viable nematode communities and whether these organisms can be morphologically characterized using SEM.

Figure 7: *E. annectens* femur portion to be ground sectioned (in preparation). Scale marker=11cm on each side.

Figure 8: Baermann funnel set up for live nematode extraction from *E. annectens* femur fragments.

Materials and Methods

E. *annectens* disarticulated bone fragments were collected to examine for living nematodes at a mono-dominant assemblage site [31] in the Lance Formation, (Hansen Ranch) near Newcastle, WY on two different dates in June, 2025 (Figures 6 and 7). We (authors MA, KH) took multiple bone fragments from the large femur, which was partially exposed at 0–10cm depth (Figure 6). Another four sets of bone (not pictured) were collected (by author KP) for live nematode extraction: tooth root at 80cm depth, associated cranial bones at 63cm depth, and chevron at 13cm. Soil samples were also collected in the immediate vicinity of the second sets of bones. A large portion of the first bone sample (Figure 7) was immersed in 10% formalin at the site for ground section study (in preparation), while others were triple-bagged and transported to the lab for live worm extraction. We (authors MA, KH). also collected living worms

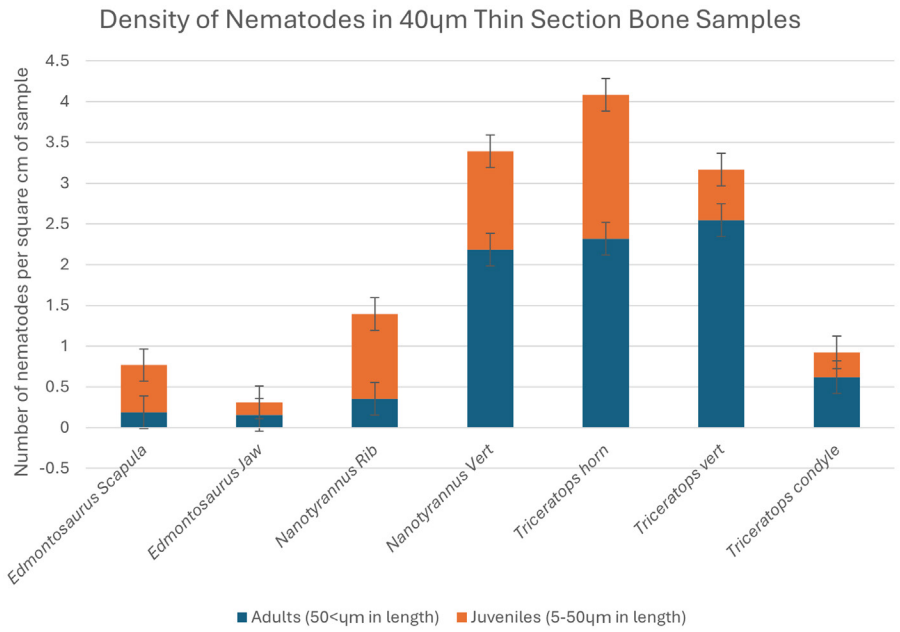

Figure 9: Density of adult and juvenile nematode populations in 40µm ground sections of dinosaur bone. Error bars=standard error.

at the site within 2 hours of disinterring them. We employed a standard Baermann setup with 75mm glass conical funnels and attached latex tubing to the funnel stems. Tubing was clamped to prevent water outflow, and funnels were stabilized in a hard plastic frame. A modified, field-ready Baermann funnel (Figure 8) was used to collect nematodes from soil and the second set of *E. annectens* bones.

Funnels with clamped tubing were filled with deionized (DI) water, and clamps were briefly opened to allow water flow, thus ensuring bubble-free tubes. Bone fragments were scrubbed by brush, rinsed with DI water several times, and placed in a double-layered Kimwipe lint-free pouch. The pouches were secured with rubber bands and completely submerged in the funnel water. 15g of soil was also placed in pouches, secured with rubber bands, and submerged completely. Nematodes migrated out of samples, through the Kimwipes, and settled at the bottom of the water column in each tube. Tubes were periodically emptied into crystallizing dishes at 24 and 48 hours.

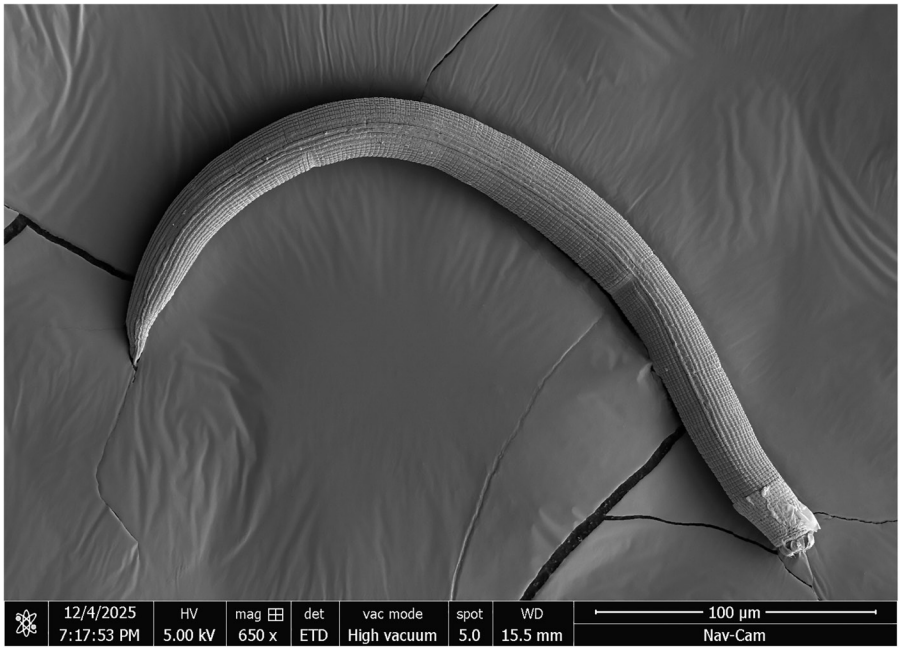

Figure 10: Unidentified living nematode, SEM (SE), extracted by Baermann funnel from *E. annectens* femur showing tail (left), cuticle striations, and cephalic lip region (right). Scale bar=100µm.

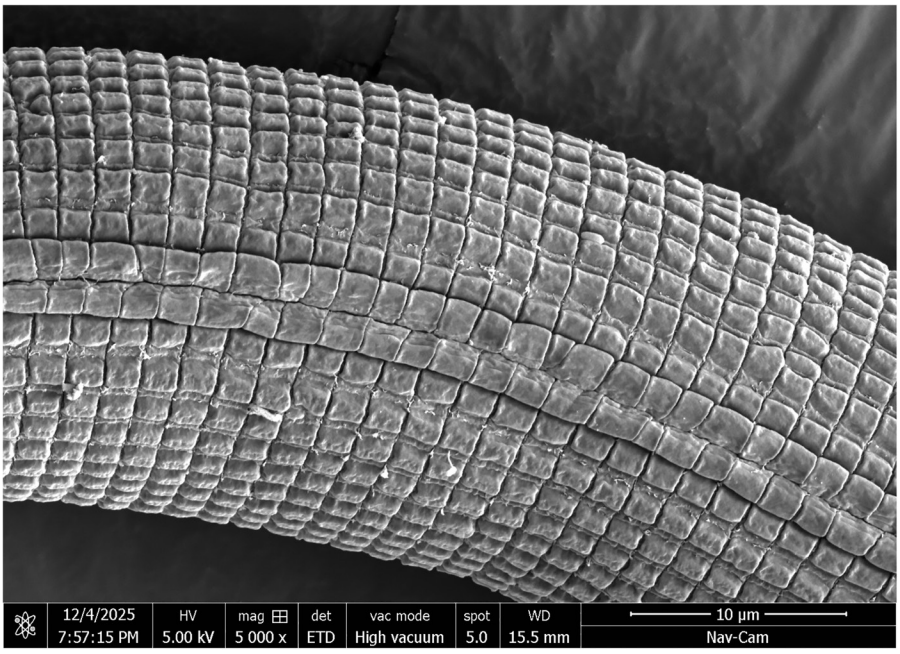

Figure 11: SEM of unidentified living nematode extracted from *E. annectens*. Cuticle detail shows lateral and transverse striations. Scale bar=10µm.

Very active worms were also successfully collected within 15 minutes of bone immersion in DI. Nematodes were pipetted into 10% formalin immediately after extraction. Then dissecting microscope video of worms in dishes (40× magnification) were collected at the site.

Nematodes were left in formalin until further processing, which included washing and fixing in 10% glutaraldehyde for 90 minutes. After another wash, worms were post-fixed in 1% osmium. Worms were dehydrated in an ethanol series, critically-point dried, and transferred to adhesive, conductive carbon-coated stubs with eyelash tools. Many worms were lost during transfer, but samples were coated in carbon and imaged with a FEI Tecnai FIB (Thermo Fisher).

Previously made 40µm ground sections of *E. annectens* and *Triceratops* (collected at Glendive, MT from 2015–2025) and *Nanotyrannus* (collected at Jordan, MT from 2021–2024) were examined using brightfield optics with a compound microscope, and nematodes in bone canals were counted using

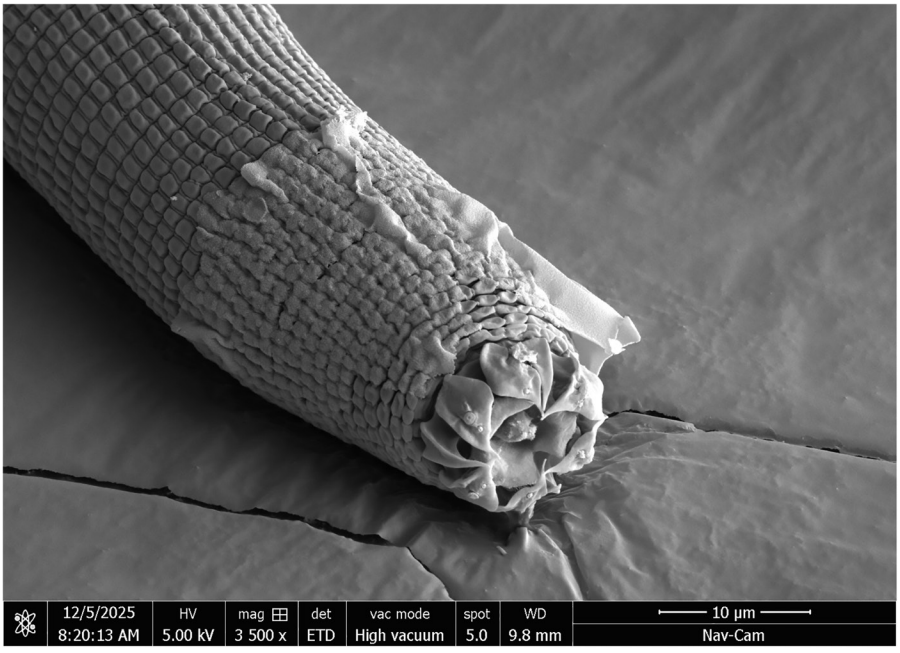

Figure 12: SEM of unidentified living nematode extracted from *E. annectens*, cephalic region. A thin veil of material circumscribes the cephalic end of the worm, obscuring some detail. Scale bar=10µm.

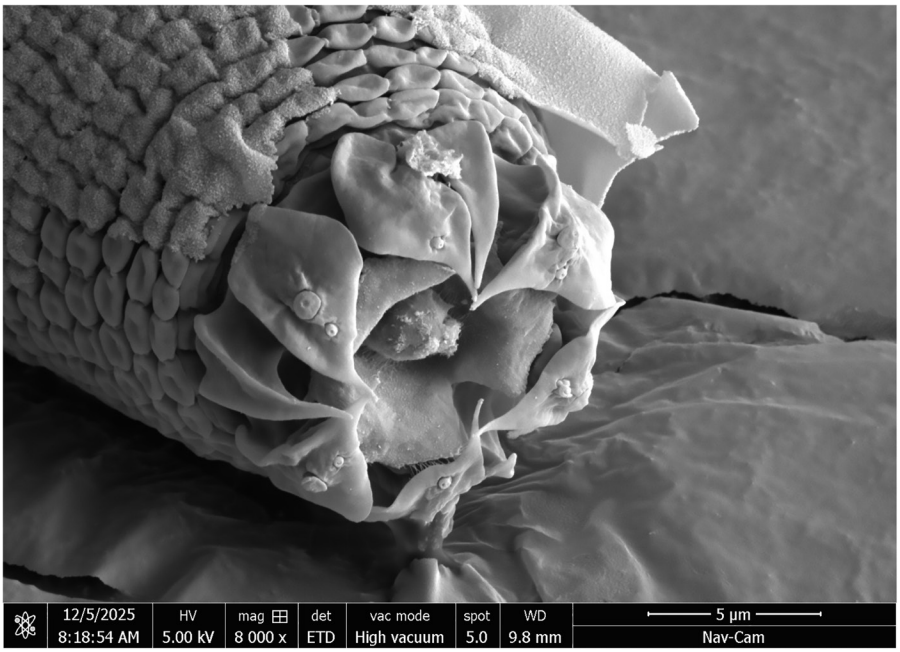

Figure 13: SEM of unidentified living nematode extracted from *E. annectens*, cephalic region. Details of the hexaradiate symmetry of the lips and sensory papillae are visible. Scale bar=5µm.

a hand-clicker. Thirty sections in total (DSTRI permanent collection) were examined, and bone surface area on each section was calculated in cm^2. Nematodes greater than 50µm in length were considered adults, and juveniles were less than 50µm in length.

Results

Nematode population analysis is shown in Figure 9. All sections contained both juvenile and adult nematodes, indicating a growing and thriving population. Population density varied widely from sample to sample with the least dense nematode populations within *E. annectens* jawbone. The densest population was found in *Triceratops* horn bone. There was no apparent correlation between population density and species of dinosaur examined. In most cases juveniles outnumbered or equaled adult population numbers. Adults had greater numbers only in *Edmontosaurus* scapula and *Nanotyrannus* vertebra.

Figure 14: SEM of unidentified soil nematode, live extracted by Baermann funnel from soil in the immediate vicinity of the *E. annectens* femur. Scale bar=50µm.

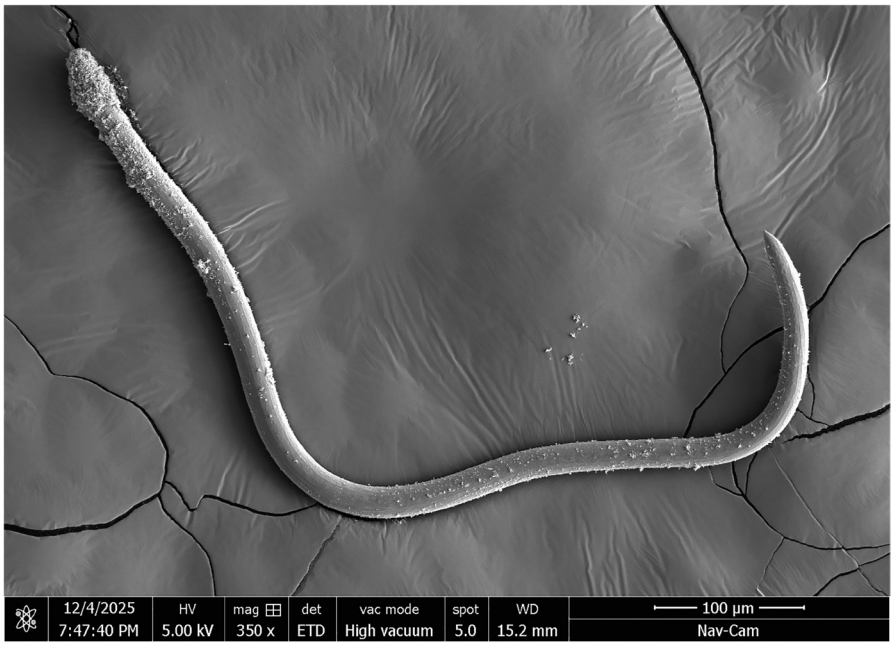

Figure 15: SEM of unidentified soil nematode, live extracted by Baermann funnel from soil in the immediate vicinity of the *E. annectens* femur. Scale bar=100µm.

Scanning electron micrographs (SEM, secondary electron imaging) of one bone worm representative is shown here (Figures 10–13). Only one bone nematode was imaged because the rest were lost (possibly during critical-point drying, in transfer, or they did not adhere to stubs properly).

Details of the cuticle pattern exhibited both transverse and longitudinal striations running the length of the body (Figure 11). Figures 12–13 provide detail of a well-preserved cephalic region displaying the characteristic hexaradiate symmetry of the six lips.

Soil worm SEM images are shown in Figures 14–17. These worms were associated with the *E. annectens* specimens and appeared to have soil contaminant still adhering to them, obscuring some structure. Diverse cuticle patterns including lateral and transverse striations with both fine and coarse annules are visible in Figure 14.

Discussion and Conclusions

Live nematodes were extracted from all soil samples (Figures 14–17) collected within the immediate vicinity of the

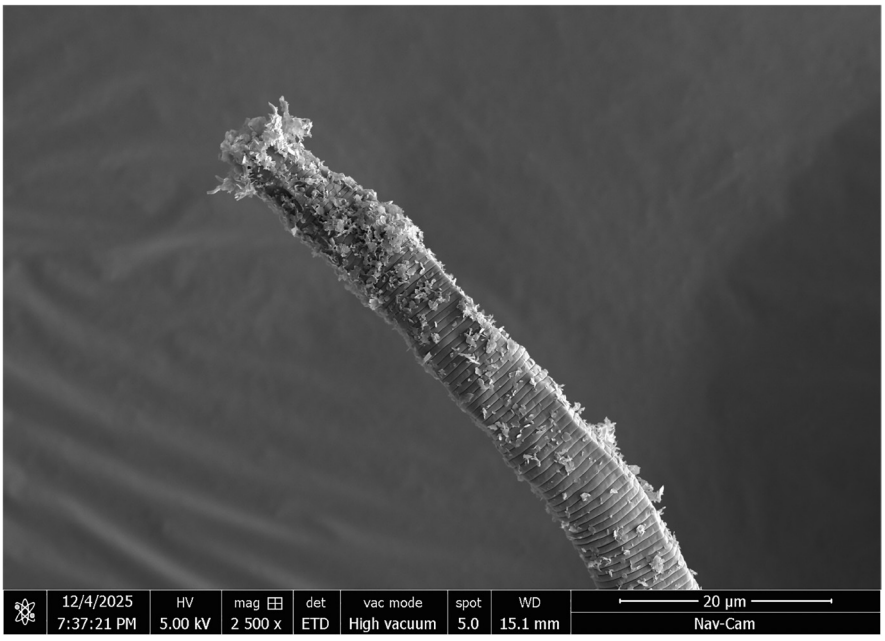

Figure 16: SEM of unidentified soil nematode, live extracted by Baermann funnel from soil in the immediate vicinity of the *E. annectens* femur. Cephalic region (on left) shows possible monhysterid setae protruding. Scale bar=20µm.

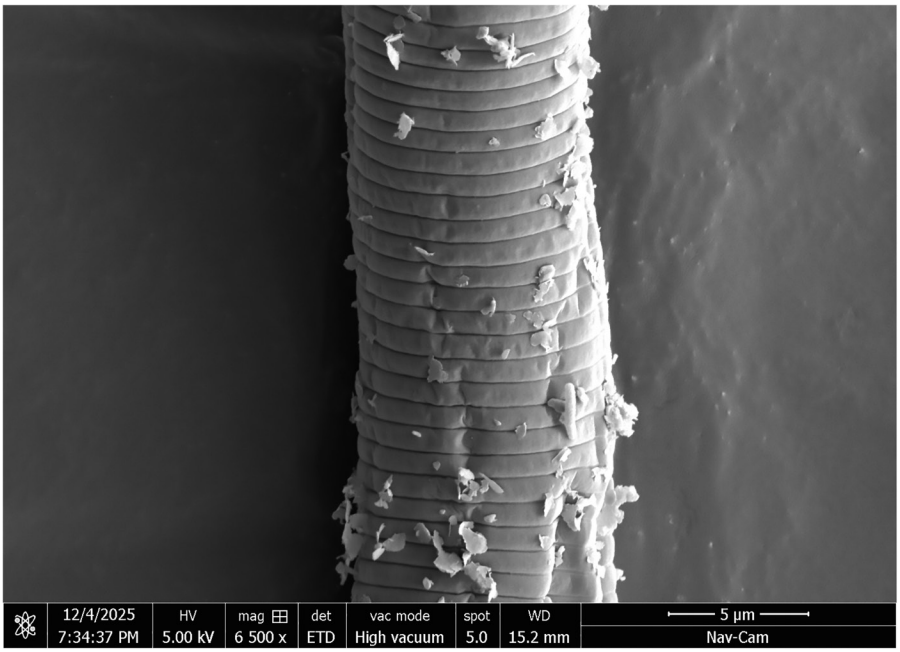

Figure 17: SEM of unidentified soil nematode, live extracted by Baermann funnel from soil in the immediate vicinity of the *E. annectens* femur. Cuticle detail showing fine transverse striations. Scale bar=5µm.

E. annectens tooth root, chevron, long bone, and associated cranial bone fragments. Only the partially buried femur fragments yielded live nematodes (n=18). Interestingly, we boosted populations of juveniles by immersing femur fragments in liquid nematode nutrient agar overnight before funnel extraction (unpublished data).

Our ability to extract nematodes directly from bone material (Figures 10–13) indicates that the fusiform-shaped nematodes observed in the ground sections (Figures 4 and 5) are, in fact, extant opportunistic decomposers, which are part of a larger decomposer community. Previous identification of extracted nematodes as fungivores (Figure 3) in addition to the fungi found in association with these bones [21,22,32] may provide clues regarding specific roles they play in the intra-bone community. More work on these communities of decomposers is warranted, and we certainly seek collaboration with those who could help identify the novel nematodes inhabiting dinosaur bone described here.

Acknowledgments

We thank Bernd Zechmann for processing and imaging insights and our colleagues at the Hanson Ranch dig site in WY (particularly John and Brenda Bollwerk, Keith Snyder, and Art Chadwick) for their kind assistance and for access to the dig. We also thank the editors at *Microscopy Today* for reviewing this work.

References

[1] RE Ingham, *Nematodes in Methods of Soil Analysis: Part 2, Microbiological and Biochemical Properties*, Soil Science Society of America, 1994, https://doi.org/10.2136/sssabookser5.2.c22.
[2] J van den Hoogen et al., *Nature* 572 (2019) https://doi.org/10.1038/s41586-019-1418-6.
[3] T Bongers and H Ferris, *Trends Ecol Evol* 14 (1999) https://doi.org/10.1016/s0169-5347(98)01583-3.
[4] LS Taylor et al., *PloS One* 15 (2020) https://doi.org/10.1371/journal.pone.0241777.
[5] I Szelecz et al., *Soil Biol Biochem* 103 (2016) https://doi.org/10.1016/j.soilbio.2016.09.011.
[6] I Szelecz et al., *Sci Rep* 8 (2018) https://doi.org/10.1038/s41598-017-18179-z.
[7] AL Emmons et al., *PLoS ONE* 15 (2020) https://doi.org/10.1371/journal.pone.0218636.
[8] H Deel et al., *mSphere* 6 (2021) e0045521 https://doi.org/10.1128/mSphere.00455-21.
[9] GO Poinar Jr., *Revue Nematol* 7 (1984) https://horizon.documentation.ird.fr/exl-doc/pleins_textes/pleins_textes_5/pt5/nemato/15616.pdf.
[10] GO Poinar Jr. et al., *Fundam Appl Nematol* 17 (1994) https://www.researchgate.net/publication/32973952_Earliest_fossil_nematode_Mermithidae_in_Cretaceous_Lebanese_amber.
[11] GO Poinar Jr. and R Buckley, *J Invert Path* 93 (2006) https://doi.org/10.1016/j.jip.2006.04.006.
[12] GO Poinar Jr, *Nematology* 14 (2012) https://doi.org/10.1163/156854111X612199.
[13] GO Poinar Jr, *Palaeontology of Nematodes in Nematoda*, Walter de Gruyter, Berlin, 2013. ISBN: 978-3-11-027375-5.
[14] M Horrocks et al., *Archaeol Oceania* 59 (2024) https://doi.org/10.1002/arco.5342.
[15] J Tweet et al., *J Paleontol* 90 (2016) https://doi.org/10.1017/jpa.2016.43.
[16] MH Armitage, *Microsc Today* 30 (2022) https://doi.org/10.1017/S1551929522001262.
[17] MH Armitage, *Microsc Today* 32 (2024) https://doi.org/10.1093/mictod/qaad110.
[18] T Aureliano et al., *Cretaceous Res* 118 (2021) https://doi.org/10.1016/j.cretres.2020.104672.

[19] MH Schweitzer et al., *Sci Rep* 15 (2025) https://doi.org/10.1038/s41598-025-85497-y.
[20] ET Saitta et al., *eLlife* 8 (2019) https://doi.org/10.7554/eLife.46205.
[21] KA Peterson and MH Armitage, *Microsc Microanal* 31 (2025) https://doi.org/10.1093/mam/ozaf048.944.
[22] MH Armitage, *Microsc Microanal* 31 (2025) https://doi.org/10.1093/mam/ozaf048.945.
[23] KA Peterson and MH Armitage, *Tex J Micros* 56 (2025) https://dstri.org/wp-content/uploads/2025/03/TX_Soc_24_Peterso.pdf.
[24] JA Cruz and MH Armitage, *Microsc Microanal* 31 (2025) https://doi.org/10.1093/mam/ozaf048.965.
[25] MH Armitage, *Acta Hist* 115 (2013) https://dx.doi.org/10.1016/j.acthis.2013.01.001.
[26] SK Drumheller et al., *PLoS ONE* 17 (2022) https://doi.org/10.1371/journal.pone.0275240.
[27] BJN Long et al., *Proc Royal Soc A* 481 (2025) https://doi.org/10.1098/rspa.2025.0175.
[28] WW Stein, *J Paleo Sci* 8 (2019) https://www.researchgate.net/publication/339815047_TAKING_COUNT_A_Census_of_Dinosaur_Fossils_Recovered_From_the_Hell_Creek_and_Lance_Formations_Maastrichtian.
[29] PV Ullmann et al., *Chem Geol* 672 (2025) https://doi.org/10.1016/j.chemgeo.2024.122501.
[30] HN Woodward et al., *Paleobiol* 41 (2015) https://doi.org/10.1017/pab.2015.19.
[31] AM Bailleul et al., *PeerJ* 7 (2019) https://doi.org/10.7717/peerj.7764.
[32] ET Saitta et al., *bioRxiv* (2018) https://doi.org/10.1101/400176.

MT